ELSEVIER

Contents lists available at ScienceDirect

Journal of Cleaner Production

journal homepage: www.elsevier.com/locate/jclepro





Disassembly of in-plastic embedded printed electronics

Stephan Harkema ^{a,*}, Peter A. Rensing ^a, Sanne M.D.C. Domensino ^b, Joris M. Vermeijlen ^b, Diana E. Godoi Bizarro ^c, Antoinette van Schaik ^d

- ^a TNO at Holst Centre, High Tech Campus 31, 5656 AE, Eindhoven, the Netherlands
- ^b Fontys University of Applied Sciences, Rachelsmolen 1, 5612 MA, Eindhoven, the Netherlands
- ^c TNO Circularity & Sustainability Impact, Princetonlaan 6, 3584 CB, Utrecht, the Netherlands
- ^d MARAS B.V., Rijsbes 46, 2498 AS, Den Haag, the Netherlands

ARTICLE INFO

Handling Editor: Mingzhou Jin

Keywords: Electronics Circular economy Metals Carbon footprint Disassembly Eco-design

ABSTRACT

We explored a novel design-for-recycling method for encapsulated printed electronics in an injection-molded package that improves disassembly at End-of-Life (EoL). To this end, a non-adhering disassembly layer (NADL) was applied onto the printed circuitry and light-emitting diodes prior to injection molding. Surprisingly, the devices with a disassembly layer remained fully functional after injection molding, despite exposure to high shear forces and elevated temperatures. Facilitating the disassembly of an encapsulated electronic device using a weak link in the adhesion strength of the overmolded encapsulant invokes a contradiction: the possibility to remove the injected plastic from any underlying coating goes against the requirement of high adhesion over the entire surface area for structural strength and integrity during the harsh conditions expected by industry. To achieve balance between disassemblability and reliability, the adhesion strength of the overmolded encapsulant was tuned using vias in the coating design. To the author's best knowledge, this is the first time design-forrecycling principles were successfully applied to such in-mold structural electronics devices. Accelerated lifetime tests at 85 °C/85% relative humidity for 1000 consecutive hours were conducted to study the reliability of devices realized with this design-for-recycling method. Mechanical disassembly of molded devices proceeded uniformly along the intended interface of NADL with molded polycarbonate resin and exposed the printed Ag and surface-mounted components, thereby demonstrating the possibility to perform subsequent and dedicated recycling on plastics and metals separately.

1. Introduction

The printed circuit board (PCB) has matured into a reliable backbone for modern-age technology. With the deteriorating state of the global climate, concerns are mounting about the fast growing electrical and electronic equipment waste (WEEE), most of which contains PCBs, from around 42 million tons in 2014 to around 65 million tons in 2017 (Cesaro et al., 2018). PCBs accounted for 1.2 million tons of e-waste, of which around 34% are recycled by environmentally sound facilities, according to the Global Transboundary E-waste Flows Monitor in 2022. This percentage is higher than the average of WEEE due to high amount and value of the metal content (Attah-Kyei et al., 2020; Cucchiella et al., 2015; Ghosh et al., 2015). An example PCB from a personal computer contains on average 7% Fe, 5% Al, 20% Cu, 1.5% Pb, 1% Ni, 3% Sn and 25% organic materials, as well as 250 ppm Au, 1000 ppm Ag and 100 ppm Pd(Reuter et al., 2013). In addition to the presence of the

non-metallic content, the complex multi-material composition of PCBs and the combination of non-compatible metals/metallic compounds lead to limited recycling rates (Ghosh et al., 2015; Reuter et al., 2013). Due to the increasing complexity of electronics and electronic devices, a product-centric approach to recycling, as opposed to material-centric, would be much more appropriate as it considers complex interactions in a recycling system(Reuter et al., 2013). It is becoming abundantly clear that recycling is a necessity for uncompromised sustainability and that future technologies, e.g. those based on printed electronics, need to incorporate materials, techniques, and designs that further reduce the overall environmental impact, facilitate full recycling, and find their place in a circular economy.

Thanks to advances in the past decades, printed electronics (PE) form an even more preferred alternative to PCBs, especially considering the environmental aspects (Gehring et al., 2021; Liu et al., 2014; Prenzel et al., 2021; Wiklund et al., 2021). Printing of metals for electronic

E-mail address: stephan.harkema@tno.nl (S. Harkema).

^{*} Corresponding author.

components was developed in the mid-twentieth century and gained considerable traction for ceramic capacitors using nickel nanoparticle ink and aluminum busbars in silicon solar cells (Suganuma, 2014). More recently, printed electronics were studied for flexible RFID sensors (Baumbauer et al., 2020; Subramanian et al., 2005), as a replacement for discrete SMD components (for instance capacitive touch sensors (Barrett and Omote, 2010; Salim and Lim, 2017), and pressure sensors (Lozano Montero et al., 2021)), lighting foils (Keränen et al., 2015; Van Den Ende et al., 2012), medical wearable devices (Campero Jurado et al., 2023; Sreenilayam et al., 2020), and as replacements for printed circuit boards (Eshkeiti et al., 2015; Phung et al., 2021a, 2021b). As such, printed electronics can be found in various domains including automotive, consumer electronics, and more recently wearables and healthcare. Depending on the nature of the often thermoplastic substrate, printed-electronics devices may benefit greatly from the substrate's inherent flexibility, stretchability, formability, wearability, biocompatibility, and associated reduced thickness and weight in comparison to conventional PCBs. Additive printing of metal inks at low cost to form thin-film circuitry is a unique selling point of printed electronics (Suganuma, 2014), whereas the conventional printed circuit boards require multiple copper deposition and etching steps. To overcome (printed) metal corrosion (Boda et al., 2023; Graedel, 1992; Huang et al., 2020), scratching of metal tracks and other forms of damage, both PCBs and printed electronics are partially or fully encapsulated (Phung et al., 2021a). This improves weatherability, durability and scratch resistance, but creates a significant challenge at End-of-Life (EoL) to recycle such in-plastic embedded electronics.

Printed electronics are perceived as a green technology (Gehring et al., 2021; Kokare et al., 2022; Liu et al., 2014; Nassajfar et al., 2021; Prenzel et al., 2021; Välimäki et al., 2020; Wiklund et al., 2021). Nevertheless, few direct comparisons between products based on printed electronics and on conventional PCBs are available. For printed-electronics devices close to industrialization, recent life-cycle assessments for in-molded structural electronics (IMSE) showed reductions of the carbon footprint by 34% for an automotive control panel and 20-31% for a coffee machine control panel (Jääskä et al., 2023; Jääskä and Muñoz, 2022). The latter coffee-machine panel was designed to replace a near-identical coffee-machine panel based on a PCB. The largest reduction in CO₂ footprint (31%) was obtained when omitting the external driving electronics and replacing it with a system-in-package component that is fully included within the injection-molded cavity (Jääskä et al., 2023). The use of bio-based, recycled materials and/or metals with a lower environmental impact may lead to further improvements. Exceptionally high reductions to the environmental impacts were determined in 2014 by Liu et al. for a three-layer paper-based PCB in comparison to a four-layer conventional PCB reference. A factor 71 reduction in global warming potential (GWP) was obtained in addition to at least a factor 65 reduction to the other impact categories that were included (Liu et al., 2014). More recently, Nassajfar et al. provided an extensive LCA comparison between fiber-glass-reinforced brominated epoxy resin (FR4) substrates for PCBs and the comparative cases of PET, PLA/GF composite and paper (Nassajfar et al., 2021). A reduction of more than 85% was calculated for the GWP of each of the comparative cases. The silver nanoparticles of the printed circuitry remained as the primary hotspot for printed electronics on these substrates. A study by Sudheswar et al. provided a direct comparison of PCBs with printed electronics on paper and included a variation of the area covered by (printed) metals in the sensitivity analysis of the LCA (Sudheshwar et al., 2023a). The authors state that ensuring the recycling of Ag or only using recycled Ag in the production processes, printed electronics have a constant sustainability edge over PCBs, irrespective of the required conductive area. Ultra-thin organic photovoltaic solar cells were reported to demonstrate a reduction in the GWP of up to 85% by a combination of a different substrate (bio-based instead of petrochemical), less printed silver and a modified design (Välimäki et al., 2020). Guidelines to achieve a lower environmental

footprint for printed electronics suggested to replace silver with copper (Prenzel et al., 2021) due to its factor 70 lower impact as is described in an extensive life-cycle-assessment study for the mining of metals (Nuss and Eckelman, 2014). While this choice for a different metal would reduce the global warming potential by more than 95%, its impact is limited to the printed circuitry if processing remains otherwise identical. All these studies indicate the sustainable potential of printed electronics. To assist in decision making in the transition towards this green technology, a selection tool was developed to identify in which applications printed electronics could replace the conventional printed circuitry board (Sudheshwar et al., 2023b).

While typically less complex than PCBs, printed electronics do contain printed metals in addition to discrete semiconductor components such as sensors, actuators, capacitors, resistors, LEDs and driving chips, which harbor a multitude of metals and metallic compounds. Endof-life physical recycling (shredding and sorting) of printed electronics may produce partially un-liberated, low grade complex recyclates similar to PCBs and thus benefit from a product-centric approach to recycling (Reuter et al., 2013; Van Schaik and Reuter, 2014). While printed electronics enables a significant reduction in the environmental impact of the production phase compared to similar devices based on PCBs, a higher reduction can still be unlocked by incorporating design-for-recycling (DfR) principles. Norgren et al. applied design-for-recycling to several use cases and examined the role of a DfR in a circular economy (Norgren et al., 2020). As stated by the authors, a design-for-recycling holds the potential to increase the quantity and value of materials recovered and reused from products that have reached their end-of-life. Experiences with PCB waste may provide guidelines for printed electronics products as well. When comparing automated shredding and sorting of PC (personal computer) e-waste to manual dismantling, higher recovery rates were obtained for the latter (92% vs 75% for Ag, 97% vs 70% for Au, and 99% vs 41% for Pd) (Meskers et al., 2009). The economic viability of manual disassembly, however, may limit the available time to dismantle, as was shown in a separate study on displays (Ardente et al., 2014). Incorporating a "design for disassembly" in the production of the displays was therefore suggested to support the adoption of manual disassembly. Another study indicated that extensive dismantling and high-quality recycling would lead to the highest reduction of the product's global warming potential (Alston et al., 2011; Alston and Arnold, 2011). More recently, a study on the Fairphone 2 explains the advantages and disadvantages of a modular design with respect to recycling and offered insights into three recycling routes (Reuter et al., 2018). This study shows that a modular approach to recycling, supported by advanced disassembly/separation of components/parts into modules better matching the processing options of (metallurgical) final treatment processing, can significantly improve recycling performance.

In this publication, we explore a dedicated design-for-recycling for in-mold structural electronics that makes use of a non-adhering disassembly layer (NADL) that is capable of withstanding high temperature processing, injection molding and the harsh reliability tests that mimic the use phase. First, a detailed description of the IMSE device build-up, processing steps and processing conditions is provided in Chapter 2 along with the method used to disassemble the PC encapsulant from the PC functional substrate. Chapter 3 presents the research findings of IMSE device manufacturing, reliability tests and subsequent disassembly. Chapter 4 provides a discussion on the design-for-recycling, the disassembly process and the potential impacts of the use of a NADL on the device aesthetics, costs and end-of-life recycling. Chapter 5 provides our conclusions.

2. Experimental

2.1. In-mold structural electronics device manufacturing

In-mold structural electronics (IMSE) is a variant of printed

electronics in which printed circuitry is applied to a flat thermoplastic substrate and integrated into an object with a $2\frac{1}{2}$ or 3D-shape. It combines known production methods called In-Mold Decoration or In-Mold Labelling with an alternative approach to electronics, namely by printing wires and circuitry, and bonding SMD components onto the printed circuitry. By printing or adding discrete SMD components, such as light emitting diodes (LEDs), sensors, resistors, capacitors and driving chips, IMSE provides a great deal of added functionalities (e.g. light source, sensors, actuators). Unique to IMSE is the combination of printed electronics onto 2D substrates with high-pressure thermoforming to achieve the $2\frac{1}{2}$ or 3D shape of the final product. Subsequent injection molding provides stability, rigidity and encapsulation of printed electronics from environmental influences.

Our IMSE devices were manufactured using sheet-to-sheet processing onto a 175-micron-thick polycarbonate substrate of 390 \times 260 mm² (Makrofol DE 1-1, Covestro), onto which 2 layers of black and 2 layers of white graphic inks (Noriphan N2K 945 and 954, Proell) were separately screen printed using a Dek Horizon 03i with 250 SD mesh screen (see Figs. 1 and 2). Each printed wet layer was roughly 19 μm thick. The graphic layers were cured using a Spidé Mistral 360 conveyor reflow oven set at 85 °C, at a speed of 35 cm/min, which took approximately 5 min. Post-curing of the entire stack, as specified by the supplier, was done for 2-4 h in a box oven. On top of the stack of graphic layers, the Ag circuitry was screen printed with commercially available silver ink (ME604, DuPont) at a thickness of 11–12 μ m. Following curing at 120 $^{\circ}$ C for 10 min, a transparent non-adhering disassembly layer (NADL) was screen printed using similar settings and squeegees to obtain a 16 μm thick coating after curing in a conveyor reflow oven set at 45 °C. A water-based non-adhering material S112 (Kiwo, De) was chosen as NADL for its low adhesive strength on various hydrophilic materials. To accommodate SMD components, the NADL contained openings for the 132 green (SML-P13PTT86R, Rohm) or white LEDs (SCMP13WBC8W1, Rohm) through which the LEDs were bonded using a conductive adhesive and a Mycronic My200DX-14 Pick and Place machine. Optional vias were designed for the NADL for higher adhesive strength of the encapsulant to the functional substrate. Local dispensing of the NADL at the SMD components followed to prevent (strong) adhesion to the encapsulant. The dyed NADL was chosen to track the layer's integrity during processing and subsequent dismantling. The 132 LEDs were, by design, subdivided in 4 LED strings with equal division of LEDs amongst them, leading to 4 external contacts for the LEDs and an additional capacitive touch pad for intensity control. The half-circular design of the IMSE lighting device featured no local topology and did not require thermoforming prior to encapsulation. Encapsulation was accomplished by injection molding using an Engel Victory 50 with a custom-made halfcircular mold with a 4 mm cavity, which added roughly 65g of transparent polycarbonate resin. Before this, a Trotec Speedy 300 CO₂-laser was used to reduce the size of the substrates to match the mold. The functional substrates with printed circuitry were then pre-heated just prior to injection molding to 90 °C in a box oven for 5-10 min and an additional 30-60 s in the mold, to reduce water-uptake by the waterbased NADL. The pre-dried Sabic Lexan 123R polycarbonate pellets were heated up in the injection-molding device to 300 °C and subsequently injected into the cavity at pressures between 250 and 500 bars, at a flow rate of 5 cm³/s and with a dosage volume of 30–65 cm³. A hot runner enabled further heating of the polycarbonate resin up to 330 °C. Upon injection, the flow of hot resin originated from outside the active area at the opposite edge of the external printed Ag contacts to minimize shear forces and thermal load on the printed circuitry and components. Injection-molding parameters were optimized in the ranges indicated above. During injection of the resin, after a set dosage volume, the pressure phase started with a predefined (and constant) duration of 21 s, followed by a cooling phase of 25 s. The final device build-up and shape are provided in Fig. 2. Optical and electrical inspection and measurements of the encapsulated printed electronics and LEDs followed hereafter. To examine the durability of the IMSE devices, several samples were exposed to accelerated lifetime tests at 85 $^{\circ}$ C/85% RH for 1000 h using an Espec EGNX12-7 5CWL temperature cycling chamber. Four point-probe-resistance measurements on the printed silver circuitry were performed with a Keithley 2100 series digital multimeter.

2.2. Mechanical disassembly of the injected resin

Mechanical disassembly of the injected resin proceeded by clasping the edge of the device at the external contact leads and manually peeling off the substrate over the entire length. Alternatively, peeling was achieved with a peel force tester in a more controlled manner set at a speed of 50 mm per minute. For this, a Mark 10 M7i tensile tester was adapted with a G1109 90° Peel Fixture and with a suitably sensitive detector recorded the peel strength in the range of 0–90 N. After disassembly, the Ag circuitry and SMD components of the functional substrates were still covered by the NADL that was subsequently removed by washing it in a hot water bath of 80–90 °C for 1–2 min (see also Fig. 6b).

3. Results

3.1. Device fabrication

The functional substrates for the IMSE lighting devices were made with consecutive screen printing of double layers of black and white graphic layers, silver and the non-adhering disassembly layer on top of a 175 μm -thick polycarbonate substrate. The NADL screen design contained vias for the bonding of the light-emitting diodes and optional vias designed to increase the adhesive strength of the polycarbonate over the entire active area without compromising the possibility to disassemble the device and recuperate the valuable elements, such as Ag and LEDs. Roughly 320 additional vias of 1 mm in diameter were added to a few devices to support the overall structural strength of the part in addition to the 5 mm-wide edges (see Figs. 1 and 3). Following bonding and optionally glob topping the LEDs with the NADL material by manual dispensing, the devices were encapsulated with polycarbonate resin through injection molding.

Injection molding followed after shortly annealing the functional substrate in an external box oven and within the mold to reduce the water uptake of the water-based NADL. Of all 10 fully functional devices included in this study, 6 devices contained the dismantling layer and 4 served as a reference. Pre-drying of this hygroscopic layer reduced its water-uptake, which resulted in a coating that appeared unaffected by the injection-molding process, as is visible in Fig. 3, and retained its fine (via) features. The presence of the NADL during bonding and injection molding did not appear to negatively affect the resistance of the 1.8 mm-wide Ag lines (7.9 \pm 0.4 Ω on average printing and curing of the silver circuitry). Measurements after injection molding, disassembly and removal of NADL with warm water provided resistance values of 2.7 \pm 0.2 Ω on average over a distance of approximately 16 mm. We attribute the decrease in resistance to additional curing during SMD bonding and injection molding.

3.2. Accelerated lifetime tests

Four devices were selected for an accelerated lifetime test in a climate chamber set at 85 $^{\circ}$ C/85% relative humidity. Two of these were reference devices without NADL. These damp heat tests did not fully follow JEDEC guidelines due to the absence of continuous or cycled bias to the printed circuitry. Such tests will be conducted in the future. While the circuitry remained functional, we did observe signs of wear during the test. First of all, we observed signs of water ingress and uptake by the NADL by discoloration (darker spots). In some cases, these

¹ JEDEC standard JESD22-A101D.01 for Steady-State Temperature-Humidity Bias Life Test, EDEC Solid State Technology Association 2021.

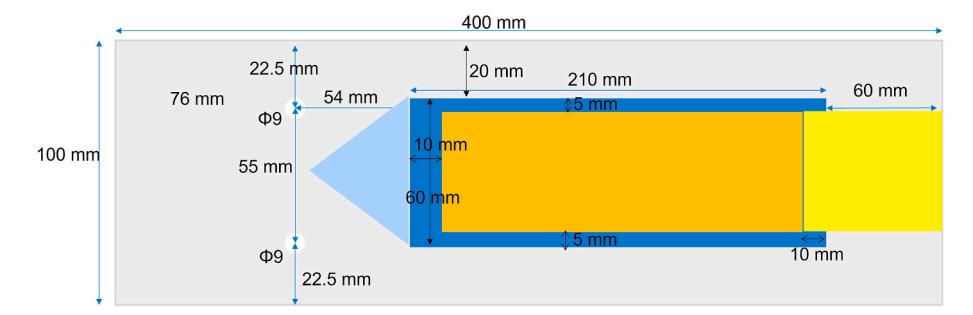


Fig. 1. Design of the IMSE lighting devices with lateral dimensions for 2D processing the functional foil; yellow corresponds to the contact area; the area in dark-blue, light blue and orange is over-molded with polycarbonate resin; orange corresponds to the functional area that is covered by NADL and contains light-emitting diodes, printed circuitry and a capacitive touch button; at the tip of the light-blue area, the polycarbonate is injected and allowed to spread evenly before flowing over printed graphic layers and circuitry. (For interpretation of the references to color in this figure legend, the reader is referred to the Web version of this article.)

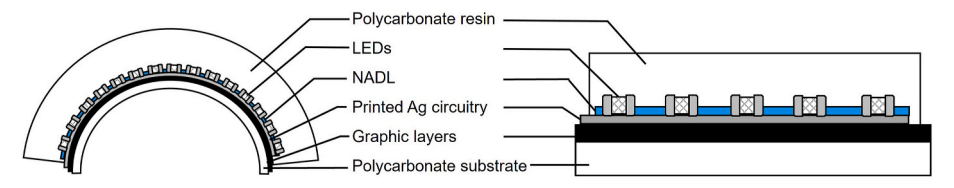


Fig. 2. Device lay-out of our in-molded lighting device. The NADL is indicated in blue and covers the printed Ag circuitry, as well as the LEDs when applied as glob top. (For interpretation of the references to color in this figure legend, the reader is referred to the Web version of this article.)





Fig. 3. Top view of the printed and injection-molded devices on 175 μm polycarbonate in its on-state with a capacitive touch button and 4 main strings of LEDs that split into 3 lines with 11 LEDs each. The blue dyed NADL in b) covers the circuitry and contains openings for the LEDs. 1 mm vias provide additional adhesion of the injected polycarbonate resin to the substrate. Additional glob tops may be applied on top of the LEDs. (For interpretation of the references to color in this figure legend, the reader is referred to the Web version of this article.).

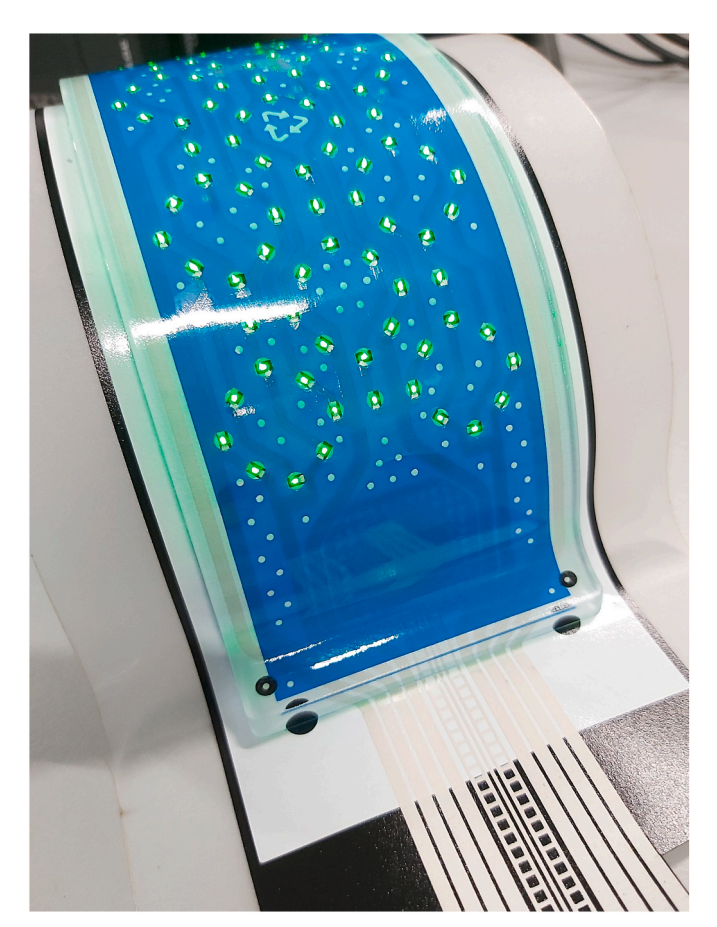
developed into blisters that locally delaminated the substrate from the injected polycarbonate resin, while the sample overall remained intact. The blisters were dynamic and were not found to be consistent. Surprisingly, some vanished over time, while others remained visible. We also observed that the polycarbonate substrate, where it extended beyond the over-molded resin, would show signs of hydrolysis in the form of stress cracking. This would occur particularly at the strong curvature at the edge of the over-molded resin. Stress cracking would extend from the edge of the substrate inwards but would halt at the edge of the over-molded resin. Cutting the substrate at the edge of the overmolded resin should resolve stress cracking in the thin PC substrate. Additional discoloration of the circuitry, a slight oxidation of the silver as visible in the reference devices, was obscured in the samples by the blue dye in the NADL and did not impact the device's functioning. The external contacts of the picture in Fig. 4 taken after 985 h also reveal this darker, silver-oxide skin.

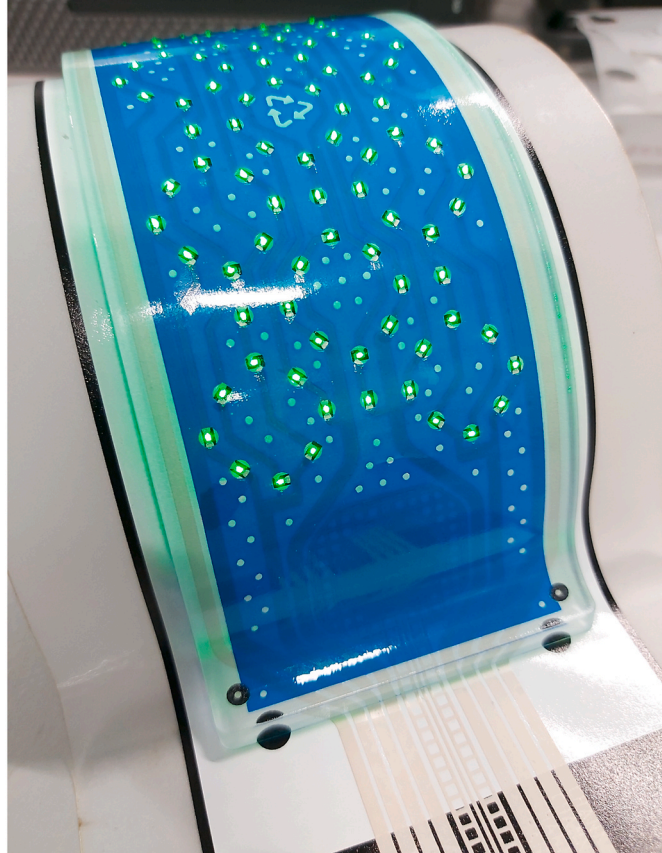
3.3. Device disassembly

Circular manufacturing requires high purity of recyclate streams and recycling products of any material involved in the fabrication and assembly of the electronics part. Valuable metals and discrete SMD components that contain rare and critical metals (Franz and Wenzl, 2017), should be recuperated as much as possible as these multi-material/complex functional components significantly complicate recycling. For optimal recovery/recycling, metallurgical (in)compatibility between metals and metal compounds, as depicted in the Metal Wheel by Reuter et al., should be considered when separating different parts/components (Reuter et al., 2013; Van Schaik and Reuter, 2014). Each segment in the Metal Wheel is representing a full metallurgical recycling infrastructure for the processing of the different (base and

associated) metals of both pyro- and hydrometallurgical processing and refining. Recycling of polycarbonate, printed silver and the LEDs from the IMSE devices in this study is thus aided considerably by liberating these from the encapsulating plastic. Ideally, these in-molded devices are dismantled at the interface of silver and over-molded plastic. In our study, the NADL serves this purpose and enables dismantling at this interface with a peel force that is tunable according to the design of the coating. The vias in the coating form ankers between encapsulant and substrate that succumb to external mechanical forces much more readily than a large area homogeneous coverage. Moreover, the density of the vias and their diameters are more easily tuned than the adhesive strength of an injection-molded resin to a specific surface. Using a separate test without printed circuitry and components (Fig. 5), it was determined that the circular vias formed by polycarbonate resin onto the Noriphan N2K graphic layer locally increased the peel strength from ~0 N up to \sim 25 N over a width of 6 cm. Vias with a diameter of 8, 4 and 2 mm correspond to patterns 3, 2 and 1, respectively. The total area of the vias per cm² was kept constant. Pattern 0 was the reference that provided no additional peel strength (~0 N). In later designs, the NADL was omitted at the periphery of the entire device to provide sufficient side encapsulation and to avoid a premature onset of disassembly.

Fig. 6a) shows an injected part that cleanly delaminated at NADL interface with PC upon mechanical dismantling. However, this is not the case at the designated areas for encapsulation (5 mm rims), the vias (none in Fig. 6) and at the SMD components in case no glob tops were applied, resulting in also ripping off the LEDs from the substrate. At these locations, the set of two black ink layers provided the weakest mechanical link, except where the silver circuitry extended beyond the NADL-covered area. The resistance of the silver at this location showed a higher value relative to the area covered with NADL (4.4 \pm 0.7 Ω vs 2.7 \pm 0.2 Ω). To avoid trapping the LEDs within the polycarbonate, glob tops





 $\textbf{Fig. 4.} \ \ \textbf{Example device with NADL after a) 48, b) 144 \ and \ c) 985 \ h \ in \ a \ climate \ chamber \ set \ at \ 85 \ ^{\circ}C \ and \ 85 \ \% \ relative \ humidity.$

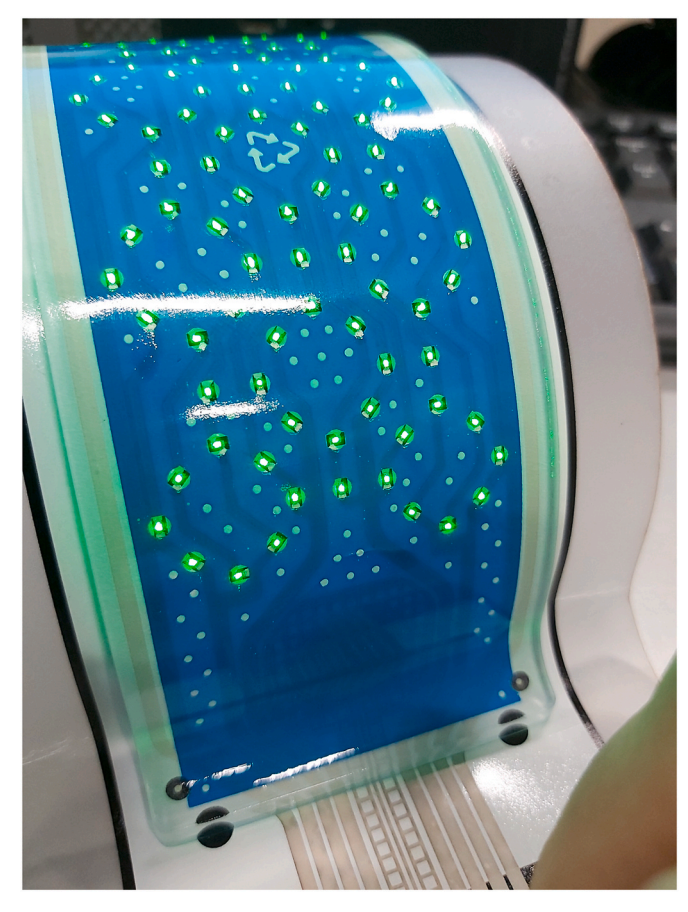


Fig. 4. (continued).

were included in other samples by dispensing the NADL material onto each LED separately. After disassembly, the water-based coating remained on both the functional substrate and LEDs and required removal. Dissolution in water proved easy immediately after screen printing and drying but required a slight temperature elevation after a few high-temperature processing steps, which included curing the isotropic-conductive adhesive for LED bonding, underfilling these with an epoxy-based adhesive and injection molding (Fig. 6b). Room-temperature removal of an NADL cured at 180 °C for 10 min was unsuccessful (outcome of 0) and demonstrates the surprisingly large impact of residual water in the layer on its properties and the subsequent resistance from re-uptake of water after thorough curing.

In the case that the device in Fig. 6a) contained glob tops on each LED separately in addition to the full area coating, the polycarbonate resin is unable to bond directly onto the components. This extent of device design and disassembly enabled the recuperation of a fully functional substrate, as shown in Fig. 7, and may be sufficient to enable a process aimed at repairing. The polycarbonate encapsulant was retrieved with only minimal surface-area contamination, stemming mostly from graphic inks (edge encapsulation, vias and the central recycling icon). The NADL coating did not reach the edge of the encapsulant, leading to minimal Ag contamination, which is preventable in a design where Ag is fully covered in the NADL-coated area.

4. Discussion

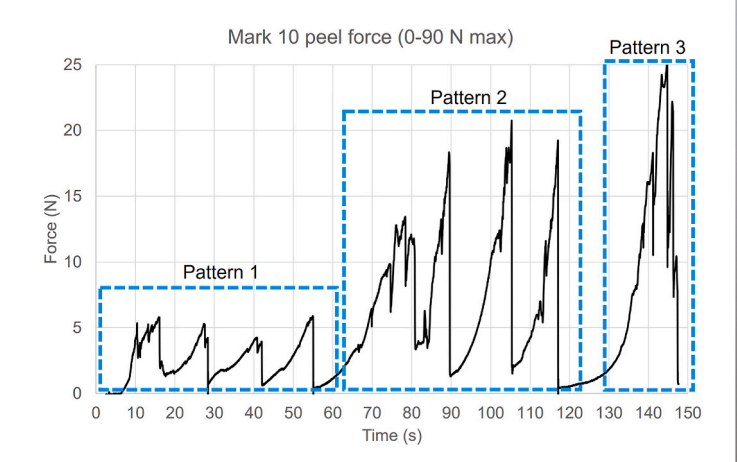
In-plastics-embedded in-mold structural electronics devices containing printed Ag and surface-mounted devices were fabricated with an additional disassembly layer intended to facilitate device disassembly for the purpose of improving recyclability. A water-soluble material was used as NADL due to its low adhesion strength when combined with

injection-molded polycarbonate. The addition of the dismantling layer has several consequences for the product itself, but also for subsequent recycling and its overall impact.

4.1. Impact of NADL on device costs and aesthetics

The aesthetics of the device were not impaired/affected by the addition of the dismantling layer when it was added to the device in a colorless form. Device fabrication proceeded as normal using injection molding of polycarbonate onto the functional substrate with printed circuitry and components. The NADL was positioned as the final layer between the printed circuitry and molded PC resin and remained undamaged during the injection-molding process despite high temperatures and high shear forces (see Fig. 2).

Additional costs of a product involving an additional dismantling layer are, in part, related to ink type and composition of the polymer, and in part to processing an additional layer. The commercial price of a NADL-type material differs from supplier to supplier, but were low in our example. Our current implementation was based on a material that had a low volume price in the order of 100 Eur/L. One liter corresponds to roughly 25–26 m² of coated area using our printing settings, leading to an increase in material usage costing ~4 Eur/m² and roughly 4.5 Euro cents for the surface area in the devices explored in our study. On an industrial scale with high-volume prices this is expected to be lower. The presence of an additional layer does add a printing and curing step to the processing, which slightly increases the power consumption, estimated at 0.02 kWh per device, increases material usage and may overall cause a slight reduction of production yield due to a non-unity yield per production step. As such, a small increase in the costs related to production is expected, however, it is beyond our means to calculate this for industrial manufacturing.



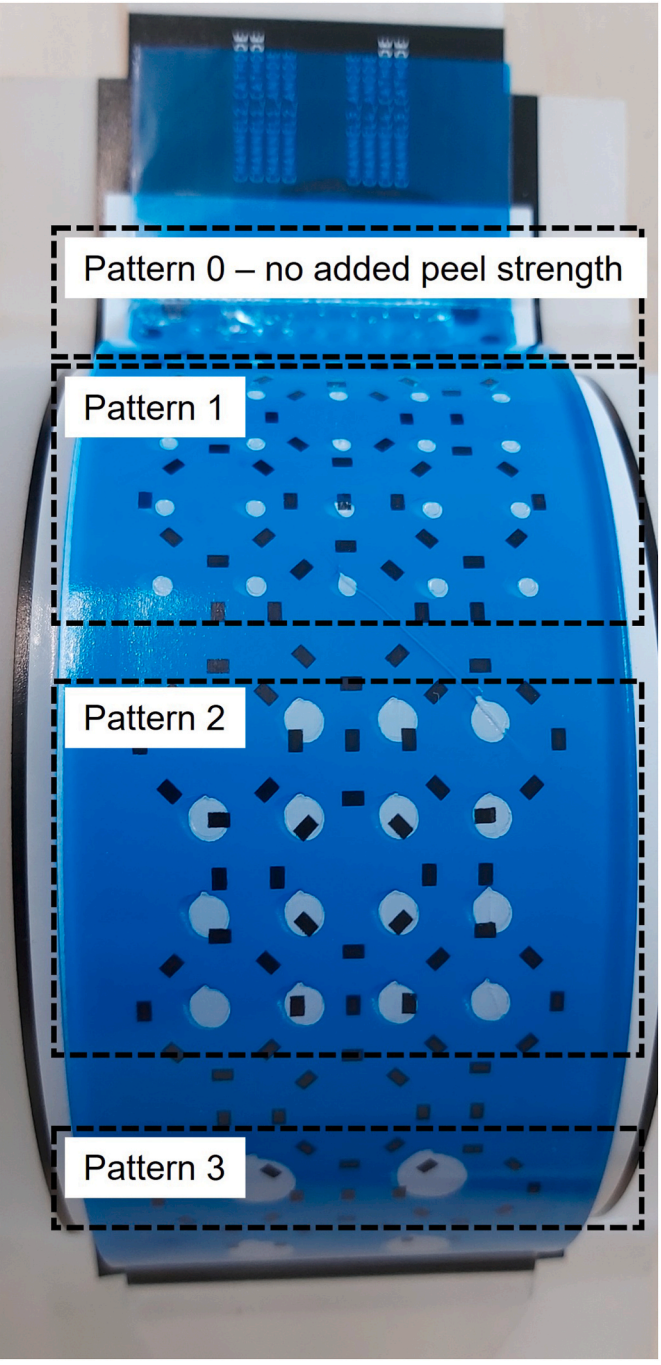


Fig. 5. a) Measured peel strength with a variation of the diameter of the vias in the NADL. The density of the via area per segment was kept constant. No side encapsulation was included as to focus on the adhesion strength provided by the vias, b) photograph of an in-molded device with patterns of vias with an increasing diameter.

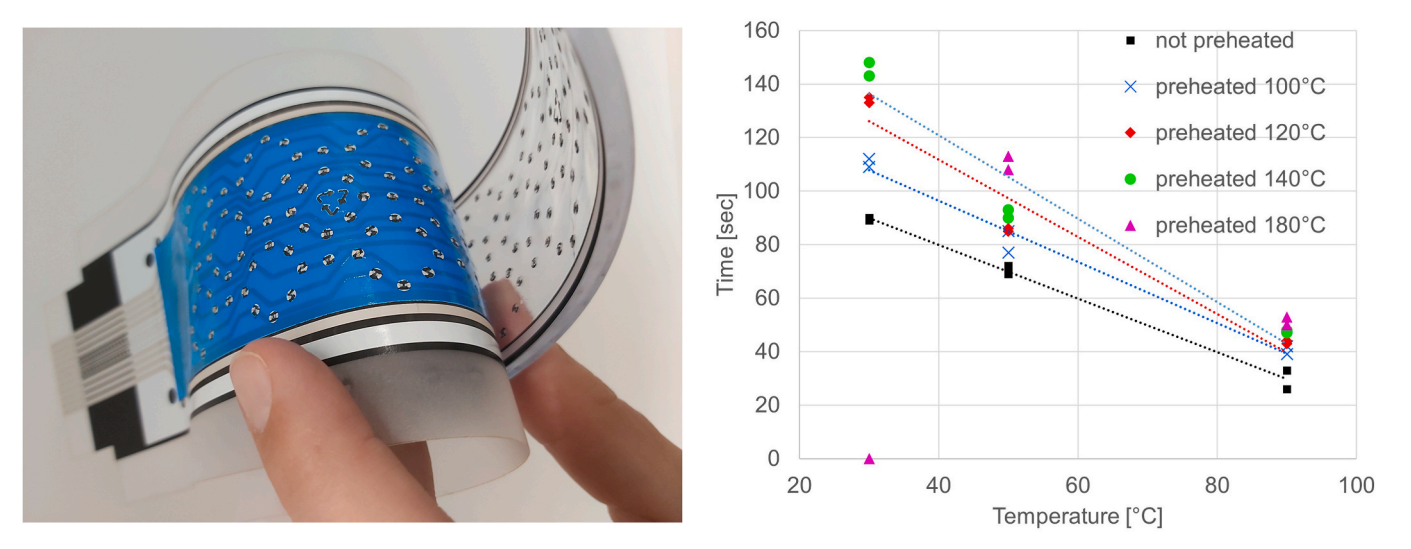


Fig. 6. a) Disassembly of an IMSE part with a blue dyed NADL, without glob tops, separating the functional substrate from the injected part, but still trapping the LEDs within the injected PC resin, b) dissolution times for the NADL in water after various heating steps. (For interpretation of the references to color in this figure legend, the reader is referred to the Web version of this article.).

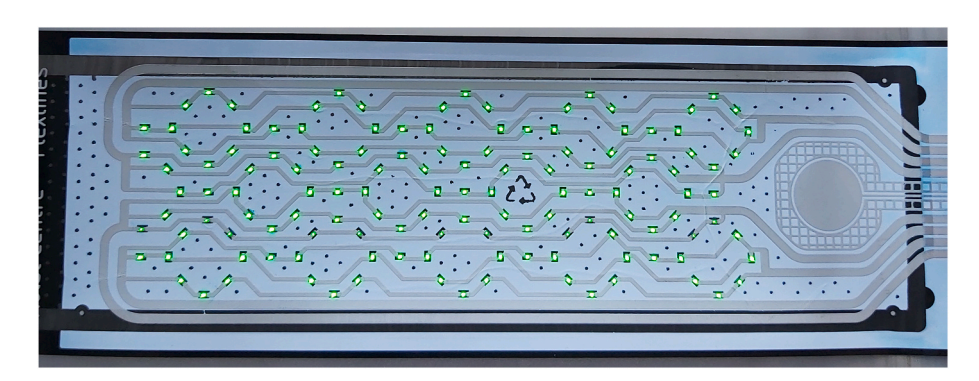


Fig. 7. Fully functional substrate obtained after disassembly using a non-adhering dismantling layer and glob tops on the light-emitting diodes.

4.2. Impact of NADL on device reliability

Designs-for-recycling that incorporate features that facilitate product disassembly and potentially improves recycling, may involve a balancing act of product reliability and improved sustainability. While reliability tests were performed in this study under the harsh conditions that are specified by the automotive industry, and results indicated that the reliability was not negatively affected by the presence of the NADL, other form factors of the devices, other graphical inks and different formulations of the NADL may affect the outcome. The devices described here were found to stay structurally intact, however, it was noted that the 175 µm-thick polycarbonate substrate suffered from stress-induced cracking due to hydrolysis during the 85 °C/85% RH test. Stress cracking of the PC that was not over-molded reveals the sensitivity of the PC to moisture and temperature, but also the severity of the conditions during this test. Any failure within the devices was not found to be related to the presence of the NADL, which is a very promising and hopeful outcome. The additional water-resistance resulting from various high-temperature steps in succession may have provided this surprising outcome when using a water-based NADL in in-mold structural electronic devices.

4.3. Environmental considerations related to the water-based NADL

The use of a dismantling layer is expected to also increase the

environmental impact in a cradle-to-gate lifecycle analysis due to the addition of a material, processing steps and a potentially lower production yield. Since the NADL was commercially obtained, we could not assess the impacts in detail, as it requires an analysis of the composition. Based on the initial solubility of the coating, we hypothesize that the material resembles a polyvinyl alcohol (PVA) as used in hydrofoils surrounding dishwasher tablets. Solubility of polyvinyl alcohols depends on the degree of hydrolysis and molecular weight (Tian et al., 2022). Since we have no indications that the material was made with bio-based materials, a petrochemical origin needs to be considered. PVA suppliers reported a global warming potential between 2.5 and 6.8 kg CO₂ eq. per kg of PVA and based these values on their own cradle-to-gate life cycle assessments (Kuraray Co. Ltd, 2022; Sekisui Chemical Company, 2018). Claims were made regarding inherent biodegradability in the aqueous dissolved form, however, this was not further elaborated on (Kuraray Co. Ltd, 2022). A cradle-to-gate life cycle assessment by Anthony et al. resulted in a value of \sim 5.6 kg CO_2 eq. per kg of PVA (Anthony et al., 2017), while in a study on the environmental impact of wood bioadhesives a value for PVA of ~2.1-2.2 kg CO₂ eq. was used (Arias et al., 2021). A low environmental impact of our NADL in combination with biodegradability would have been ideal, however, a recent marine biodegradability study shows that the biodegradability may be low to negligible (Alonso-Lopez et al., 2021). Polyvinyl alcohol is described as a water-soluble synthetic polymer that can be degraded biologically under aerobic and anaerobic conditions, however, its

degradation rate is low, especially under anaerobic conditions(Bátori et al., 2018). Bio-degradability in soil or when exposed to specific enzymes may be improved by combining polyvinyl alcohol with e.g. starch (Abdullah and Dong, 2019) or epoxidized soybean oil (Acik, 2019). While it is still prudent to avoid waste during the recycling process coming from the NADL by recovering the material as much as possible, the use of a water-soluble and bio-degradable polymer still seems desirable over the use of solvent-based dismantling layers that may have a high environmental impact and require the use of toxic solvents. Use of non-toxic solvents is typically preferred and should lead to lower emissions as well as lower impact on human health. Exact impact figures, however, are hard to provide for the steps during a recycling process and require dedicated LCA studies for the process with organic solvents in comparison to water, which was beyond the scope of our study that focused more on the technical feasibility of a design-for-recycling for encapsulated printed electronics.

4.4. Purity of PC upon disassembly

To prove that this eco-design could contribute to reducing the environmental impact of in-plastics-embedded printed electronics. initial dismantling tests were conducted. Dismantling of the injected PC resin, which corresponds to roughly 90% of the total weight of polymer in the device, was done manually and additionally by means of an adapted tensile tester. The initiation of dismantling required the highest force, due to the designed encapsulation edges, but once past the edge, a tunable amount of force was required to expose the interface of the NADL. A washing step with water removed the NADL and provided access to the printed Ag circuitry. It proved possible to remove the injection-molded polycarbonate without disconnecting LEDs from the printed circuitry when using glob tops made of the same NADL material. Disassembly did not prevent the PC encapsulant from contracting some graphic ink contaminants. While we found it was possible to avoid that Ag and the SMD components polluted the PC encapsulant, small sections of the graphic ink were torn off during disassembly. In our design, we provided structural strength to the IMSE part via 5 mm edges and vias within the functional area. These allowed direct bonding of the PC resin with the printed graphic inks on the PC substrate. Upon dismantling, the graphic coatings delaminated at the interface of the two black graphic layers at the location of the side encapsulation and vias, thereby resulting in a minimal contamination of the PC resin of less than 0.5 vol-%. It is not known how much this contamination adds to the decrease in PC properties upon thermomechanical recycling. A few reproduction cycles are expected to be feasible with a relatively small decrease in some mechanical properties, based on work by Pérez (Pérez et al., 2010), but a full study on the possibilities to re-use the dismantled PC encapsulant has not been concluded.

4.5. End-of-life recycling scenarios enabled by dismantling

Our expectation of a reduced overall environmental impact in a cradle-to-grave, or potentially in a cradle-to-cradle lifecycle analysis, comes from the potential end-of-life scenarios other than shredding and subsequent metallurgy at economy of scale, which sacrifices the plastics as an energy carrier or reductant in the metallurgic recovery process. With the possibility of dismantling IMSE, options become available to target the metals in the circuitry and semiconductor components specifically for recycling, by whatever method is most efficient/economically viable, while also preserving the plastics. The potential for higher recycling rates/efficiency upon dismantling is supported by the literature on PCB recycling, as described in the introduction section. One scenario is to shred and recover the metals from the IMSE (current default) with a loss of all organic materials. An alternative scenario we believe we enable with our approach is to dismantle and recover most of the plastic, 90% of the polycarbonate by weight that corresponds to the encapsulant, and process the functional substrate, 10% by weight of the

polycarbonate, in the metallurgic recovery route. The components can even be separated from the substrate after disassembly by mechanical force, if needed. In this scenario, we recover the same number of metals as in the first case, but significantly more plastics as well. If the polymer can be retrieved in a pure form, closed-loop recycling and manufacturing become realistic. Another alternative revolves around recycling of the printed metal on the substrate immediately after dismantling, followed by recycling of all of the plastics. Which scenario is preferred and what the overall costs/benefits are, is unknown to us at this stage of our research but is a topic for future work. The assessment and optimization of different recycling options covers pyro- and hydrometallurgical processing and refining, pyrolysis and calcination processes, and can also include newly developed processes. The assessment of recycling options linked to and combined with dismantling and PC recycling options will be performed on a rigorous recycling process simulation-based approach (Reuter et al., 2013, 2018; Van Schaik and Reuter, 2014) which allows for comparison and optimization of various recycling routes. Not only will this approach quantify material recycling and energy recovery but will provide at the same time energy and exergy indicators, which provide a physics basis for environmental and sustainability assessment. Including energy is rather important to analyze the true losses also in terms of thermodynamics of all materials, i.e., in terms of exergetic dissipation or losses in line with the second law of thermodynamics which is required to fully understand the circular economy of products and their recyclability.

5. Conclusions

In this study, a design-for-recycling method was applied to in-mold structural electronics by incorporating a water-based coating onto the silver circuitry onto which the injection-molded encapsulant poorly adhered. The tuning of the structural integrity of the entire device was achieved by a design for this non-adhering dismantling layer that featured 5 mm edges at all sides and optional vias within the encapsulated area. Accelerated aging tests in a climate chamber at 85 $^{\circ}\text{C}/85\%$ relative humidity for 1000 h revealed a sensitivity to the ingress of moisture, but less severely than anticipated for a water-based coating. Disassembly was achieved mechanically by hand or tensile tester and required forces significantly lower than the peel strength of the reference device that exceeded the load cell of the tensile tester (>95 N). The use of glob tops on light-emitting diodes enabled the removal of the polycarbonate encapsulant without severely damaging the printed circuitry and ICA bonds to the LEDs. With the printed circuitry exposed after disassembly, subsequent recycling may target the discrete SMD components and metals specifically, thereby potentially increasing the yield of recycling and allowing plastics to be recovered as high-quality material. Our approach provides an alternative to using the polycarbonate as an energy carrier and reductant in metallurgical processing of the IMSE parts (replacing primary resources). Furthermore, we believe that such design-for-recycling principles may lead to the possibility of repairable printed electronics in the future, thereby delivering on the promise of sustainable (printed) electronics.

CRediT authorship contribution statement

Stephan Harkema: Conceptualization, Data curation, Investigation, Methodology, Project administration, Supervision, Validation, Writing – original draft, Writing – review & editing. Peter A. Rensing: Investigation, Resources. Sanne M.D.C. Domensino: Investigation, Resources. Joris M. Vermeijlen: Investigation, Resources. Diana E. Godoi Bizarro: Writing – review & editing. Antoinette van Schaik: Writing – review & editing.

Declaration of competing interest

The authors declare that they have no known competing financial

interests or personal relationships that could have appeared to influence the work reported in this paper.

Data availability

Data will be made available on request.

Acknowledgements

TNO at Holst Centre is a research and innovation partner specialized in health technologies, flexible and wireless electronics, powered by the shared expertise of imec and TNO. This research has been funded by the Dutch Ministry of Economic Affairs, and the European Union's Horizon 2020 research and innovation program under grant agreement No 101003587 (EU Treasure project). Original electrical and injection mold design were realized in the Flexlines project that received funding from Interreg Vlaanderen-Nederland. The authors would like to gratefully acknowledge the exceptional contributions from Pit Teunissen, Jan van Delft, Jeroen Schram, Gerwin Kircher, Adri van der Waal and Margreet de Kok from Holst Centre. We also gratefully acknowledge the wonderful support by Rick Leuven and Yibo Su from Brightlands Material Center for injection molding with the Flexlines mold.

References

- Abdullah, Z.W., Dong, Y., 2019. Biodegradable and water resistant poly(vinyl) alcohol (PVA)/starch (ST)/glycerol (GL)/halloysite nanotube (HNT) nanocomposite films for sustainable food packaging. Front. Mater. 6, 1–17. https://doi.org/10.3389/ fmats 2019 00058
- Acik, G., 2019. Soybean oil modified bio-based poly(vinyl alcohol)s via ring-opening polymerization. J. Polym. Environ. 27, 2618–2623. https://doi.org/10.1007/s10924-019-01547-3.
- Alonso-Lopez, O., Lopez-Ibanez, S., Beiras, R., 2021. Assessment of toxicity and biodegradability of poly (vinyl alcohol) -based materials in marine water. Polymers 13, 1–9.
- Alston, S.M., Arnold, J.C., 2011. Environmental impact of pyrolysis of mixed WEEE plastics part 2: life cycle assessment. Environ. Sci. Technol. 45, 9386–9392.
- Alston, S.M., Clark, A.D., Arnold, J.C., Stein, B.K., 2011. Environmental impact of pyrolysis of mixed WEEE plastics part 1: experimental pyrolysis data. Environ. Sci. Technol. 45, 9380–9385. https://doi.org/10.1021/es201664h.
- Anthony, R., Sharara, M.A., Runge, T.M., Anex, R.P., 2017. Life cycle comparison of petroleum- and bio-based paper binder from distillers grains (DG). Ind. Crops Prod. 96, 1–7. https://doi.org/10.1016/j.indcrop.2016.11.014.
- Ardente, F., Mathieux, F., Recchioni, M., 2014. Recycling of electronic displays: analysis of pre-processing and potential ecodesign improvements. Resour. Conserv. Recycl. 92, 158–171. https://doi.org/10.1016/j.resconrec.2014.09.005.
- Arias, A., Feijoo, G., Moreira, M.T., 2021. Evaluation of starch as an environmental-friendly bioresource for the development of wood bioadhesives. Molecules 26. https://doi.org/10.3390/molecules26154526.
- Attah-Kyei, D., Akdogan, G., Dorfling, C., Zietsman, J., Lindberg, D., Tesfaye, F., Reynolds, Q., 2020. Investigation of waste PCB leach residue as a reducing agent in smelting processes. Miner. Eng. 156 https://doi.org/10.1016/j. mineng.2020.106489.
- Barrett, G., Omote, R., 2010. Projected-capacitive touch technology. Inf. Disp. 26 (1975), 16–21. https://doi.org/10.1002/j.2637-496x.2010.tb00229.x.
- Bátori, V., Åkesson, D., Zamani, A., Taherzadeh, M.J., Sárvári Horváth, I., 2018. Anaerobic degradation of bioplastics: a review. Waste Manag. 80, 406–413. https://doi.org/10.1016/j.wasman.2018.09.040.
- Baumbauer, C.L., Anderson, M.G., Ting, J., Sreekumar, A., Rabaey, J.M., Arias, A.C., Thielens, A., 2020. Printed, flexible, compact UHF-RFID sensor tags enabled by hybrid electronics. Sci. Rep. 10, 1–12. https://doi.org/10.1038/s41598-020-73471-9.
- Boda, U., Strandberg, J., Eriksson, J., Liu, X., Beni, V., Tybrandt, K., 2023. Screen-printed corrosion-resistant and long-term stable stretchable electronics based on AgAu microflake conductors. ACS Appl. Mater. Interfaces 15, 12372–12382. https://doi. org/10.1021/acsami.2c22199.
- Campero Jurado, I., Lorato, I., Morales, J., Fruytier, L., Stuart, S., Panditha, P., Janssen, D.M., Rossetti, N., Uzunbajakava, N., Serban, I.B., Rikken, L., de Kok, M., Vanschoren, J., Brombacher, A., 2023. Signal quality analysis for long-term ECG monitoring using a health patch in cardiac patients. Sensors 23, 1–17. https://doi.org/10.3390/s23042130.
- Cesaro, A., Marra, A., Kuchta, K., Belgiorno, V., Van Hullebusch, E.D., 2018. WEEE management in a circular economy perspective: an overview. Glob. Nest J. 20, 743–750. https://doi.org/10.30955/GNJ.002623.
- Cucchiella, F., D'Adamo, I., Lenny Koh, S.C., Rosa, P., 2015. Recycling of WEEEs: an economic assessment of present and future e-waste streams. Renew. Sustain. Energy Rev. 51, 263–272. https://doi.org/10.1016/j.rser.2015.06.010.

- Eshkeiti, A., Reddy, A.S.G., Emamian, S., Narakathu, B.B., Joyce, Michael, Joyce, Margaret, Fleming, P.D., Bazuin, B.J., Atashbar, M.Z., 2015. Screen printing of multilayered hybrid printed circuit boards on different substrates. IEEE Trans. Compon. Packag. Manuf. Technol. 5, 415–421. https://doi.org/10.1109/ TCPMT.2015.2391012.
- Franz, M., Wenzl, F.P., 2017. Critical review on life cycle inventories and environmental assessments of led-lamps. Crit. Rev. Environ. Sci. Technol. 47, 2017–2078. https:// doi.org/10.1080/10643389.2017.1370989.
- Gehring, F., Prenzel, T.M., Graf, R., Albrecht, S., 2021. Sustainability screening in the context of advanced material development for printed electronics. Mater. Technol. 109 https://doi.org/10.1051/mattech/2022013.
- Ghosh, B., Ghosh, M.K., Parhi, P., Mukherjee, P.S., Mishra, B.K., 2015. Waste Printed Circuit Boards recycling: an extensive assessment of current status. J. Clean. Prod. 94, 5–19. https://doi.org/10.1016/j.jclepro.2015.02.024.
- Graedel, T.E., 1992. Corrosion mechanisms for silver exposed to the atmosphere.
 J. Electrochem. Soc. 139, 1963–1970. https://doi.org/10.1149/1.2221162.
- Huang, H., Guo, X., Bu, F., Huang, G., 2020. Corrosion behavior of immersion silver printed circuit board copper under a thin electrolyte layer. Eng. Fail. Anal. 117, 104807 https://doi.org/10.1016/j.engfailanal.2020.104807.
- Jääskä, J., Apilo, P., Otsamo, K., Pirilä, S., Rusanen, O., Wuori, T., 2023. In-mold Structural Electronics for Sustainable Smart Surfaces [WWW Document]. https:// www.tactotek.com/resources/in-mold-structural-electronics-for-sustainable-smart -surfaces. (Accessed 10 April 2023).
- Jääskä, J., Muñoz, I., 2022. Environmental Performance of IMSE [WWW Document]. https://www.tactotek.com/resources/webinar-environmental-performance-of-imse. (Accessed 9 August 2023).
- Keränen, K., Korhonen, P., Rekilä, J., Tapaninen, O., Happonen, T., Makkonen, P., Rönkä, K., 2015. Roll-to-roll printed and assembled large area LED lighting element. Int. J. Adv. Manuf. Technol. 81, 529–536. https://doi.org/10.1007/s00170-015-7244-6
- Kokare, S., Asif, F.M.A., Mårtensson, G., Shoaib-ul-Hasan, S., Rashid, A., Roci, M., Salehi, N., 2022. A comparative life cycle assessment of stretchable and rigid electronics: a case study of cardiac monitoring devices. Int. J. Environ. Sci. Technol. 19, 3087–3102. https://doi.org/10.1007/s13762-021-03388-x.
- Kuraray Co. Ltd, 2022. All about Our Polyvinyl Alcohol (PVOH) Life Cycle Assessment [WWW Document]. URL. https://www.kuraray-poval.com/fileadmin/technical_information/brochures/poval/kuraray-poval-life-cycle-assessment.pdf, 2.4.24.
- Liu, J., Yang, C., Wu, H., Lin, Z., Zhang, Z., Wang, R., Li, B., Kang, F., Shi, L., Wong, C.P., 2014. Future paper based printed circuit boards for green electronics: fabrication and life cycle assessment. Energy Environ. Sci. 7, 3674–3682. https://doi.org/ 10.1039/c4ee01995d.
- Lozano Montero, K., Laurila, M.M., Peltokangas, M., Haapala, M., Verho, J., Oksala, N., Vehkaoja, A., Mäntysalo, M., 2021. Self-powered, ultrathin, and transparent printed pressure sensor for biosignal monitoring. ACS Appl. Electron. Mater. 3, 4362–4375. https://doi.org/10.1021/acsaelm.1c00540.
- Meskers, C.E.M., Hagelüken, C., Salhofer, S., Spitzbart, M., 2009. Impact of preprocessing routes on precious metal recovery from PCs. Proc. - Eur. Metall. Conf. EMC 2, 527–540, 2009
- Nassajfar, M.N., Deviatkin, I., Leminen, V., Horttanainen, M., 2021. Alternative materials for printed circuit board production: an environmental perspective. Sustain. Times 13. https://doi.org/10.3390/su132112126.
- Norgren, A., Carpenter, A., Heath, G., 2020. Design for recycling principles applicable to selected clean energy technologies: crystalline-silicon photovoltaic modules, electric vehicle batteries, and wind turbine blades. J. Sustain. Metall. 6, 761–774. https://doi.org/10.1007/s40831-020-00313-3.
- Nuss, P., Eckelman, M.J., 2014. Life cycle assessment of metals: a scientific synthesis. PLoS One 9, 1–12. https://doi.org/10.1371/journal.pone.0101298.
- Pérez, J.M., Vilas, J.L., Laza, J.M., Arnáiz, S., Mijangos, F., Bilbao, E., Rodríguez, M., León, L.M., 2010. Effect of reprocessing and accelerated ageing on thermal and mechanical polycarbonate properties. J. Mater. Process. Technol. 210, 727–733. https://doi.org/10.1016/j.jmatprotec.2009.12.009.
- Phung, T.H., Gafurov, A.N., Kim, I., Kim, S.Y., Kim, K.M., Lee, T.M., 2021a. IoT device fabrication using roll-to-roll printing process. Sci. Rep. 11, 1–11. https://doi.org/ 10.1038/s41598-021-99436-0.
- Phung, T.H., Jeong, J., Gafurov, A.N., Kim, I., Kim, S.Y., Chung, H.J., Kim, Y., Kim, H.J., Kim, K.M., Lee, T.M., 2021b. Hybrid fabrication of LED matrix display on multilayer flexible printed circuit board. Flex. Print. Electron. 6 https://doi.org/10.1088/2058-8585/abf5c7.
- Prenzel, T.M., Gehring, F., Fuhs, F., Albrecht, S., 2021. Influence of design properties of printed electronics on their environmental profile. Mater. Technol. 109, 1–13. https://doi.org/10.1051/mattech/2022016.
- Reuter, M.A., Hudson, C., van Schaik, A., Heiskanen, K., Meskers, C., Hagelüken, C., 2013. Metal Recycling: Opportunities, Limits, Infrastructure, A Report of the Working Group on the Global Metal Flows to the International Resource Panel.
- Reuter, M.A., van Schaik, A., Ballester, M., 2018. Limits of the circular economy: fairphone modular design pushing the limits. In: World of Metallurgy - ERZMETALL. GDMB Verlag GmbH, pp. 68–79.
- Salim, A., Lim, S., 2017. Review of recent inkjet-printed capacitive tactile sensors. Sensors 17. https://doi.org/10.3390/s17112593.
- Sekisui Chemical Company, 2018. Selvol Life Cycle Analysis [WWW Document]. https://www.sekisui-sc.com/wp-content/uploads/2020/09/07312018_selvol_lca_broch_ure_v16.pdf, 2.4.24.
- Sreenilayam, S.P., Ahad, I.U., Nicolosi, V., Acinas Garzon, V., Brabazon, D., 2020. Advanced materials of printed wearables for physiological parameter monitoring. Mater. Today 32, 147–177. https://doi.org/10.1016/j.mattod.2019.08.005.

- Subramanian, V., Fréchet, J.M.J., Chang, P.C., Huang, D.C., Lee, J.B., Molesa, S.E., Murphy, A.R., Redinger, D.R., Volkman, S.K., 2005. Progress toward development of all-printed RFID tags: materials, processes, and devices. Proc. IEEE 93, 1330–1338. https://doi.org/10.1109/JPROC.2005.850305.
- Sudheshwar, A., Malinverno, N., Hischier, R., Nowack, B., Som, C., 2023a. Resources , Conservation & Recycling the need for design-for-recycling of paper-based printed electronics – a prospective comparison with printed circuit boards. Resour. Conserv. Recycl. 189, 106757 https://doi.org/10.1016/j.resconrec.2022.106757.
- Sudheshwar, A., Malinverno, N., Hischier, R., Nowack, B., Som, C., 2023b. Identifying sustainable applications for printed electronics using the multi-perspective application selection approach. J. Clean. Prod. 383, 135532 https://doi.org/ 10.1016/j.jclepro.2022.135532.
- Suganuma, K., 2014. Introduction to Printed Electronics, first ed. Springer, New York, NY. https://doi.org/10.1007/978-1-4614-9625-0.
- Tian, G., Li, L., Li, Y., Wang, Q., 2022. Water-soluble poly(vinyl alcohol)/biomass waste composites: a new route toward ecofriendly materials. ACS Omega 7, 42515–42523. https://doi.org/10.1021/acsomega.2c05810.
- Välimäki, M.K., Sokka, L.I., Peltola, H.B., Ihme, S.S., Rokkonen, T.M.J., Kurkela, T.J., Ollila, J.T., Korhonen, A.T., Hast, J.T., 2020. Correction to: printed and hybrid integrated electronics using bio-based and recycled materials—increasing sustainability with greener materials and technologies. Int. J. Adv. Manuf. Technol. 111, 3015. https://doi.org/10.1007/s00170-020-06307-5, 3015.
- Van Den Ende, D.A., Kusters, R.H.L., Cauwe, M., Van Der Waal, A., Van Den Brand, J., 2012. Bonding bare die LEDs on PET foils for lighting applications: thermal design modeling and bonding experiments. 2012 4th Electron. Syst. Technol. Conf. ESTC 2012, 1–6. https://doi.org/10.1109/ESTC.2012.6542119.
- Van Schaik, A., Reuter, M.A., 2014. Material-centric (aluminium and copper) and product-centric (cars, WEEE, TV, lamps, batteries, catalysts) recycling and DfR rules. In: Worrell, E., Reuter, M.A. (Eds.), Handbook of Recycling. Elsevier BV, np. 360–375.
- Wiklund, J., Karakoç, A., Palko, T., Yigitler, H., Ruttik, K., Jäntti, R., Paltakari, J., 2021. A review on printed electronics: fabrication methods, inks, substrates, applications and environmental impacts. J. Manuf. Mater. Process. 5 https://doi.org/10.3390/jmmp5030089.